# Encapsulation of Thallium(I) by Tetranuclear Rhodium or Iridium Complexes: Synthesis and Molecular Structure of Heterobimetallic Complexes Stabilized by s2−d8 Bonding Interactions

**ARTICLE** *in* INORGANIC CHEMISTRY · APRIL 1999

Impact Factor: 4.76 · DOI: 10.1021/ic980988m

# Encapsulation of Thallium(I) by Tetranuclear Rhodium or Iridium Complexes: Synthesis and Molecular Structure of Heterobimetallic Complexes Stabilized by $s^2-d^8$ Bonding Interactions

**Miguel A. Casado, Jesús J. Pérez-Torrente, José A. López, Miguel A. Ciriano,* Fernando J. Lahoz, and Luis A. Oro***

Departamento de Química Inorgánica, Instituto de Ciencia de Materiales de Aragón, Universidad de Zaragoza−C.S.I.C., 50009-Zaragoza, Spain

*Received August 18, 1998*

Reactions of $[M_4(\mu\text{-}pyS_2)_2(cod)_4]$ (M = Rh, Ir; $pyS_2$ = 2,6-pyridinedithiolate, cod = 1,5-cyclooctadiene) with equimolar amounts of $TlPF_6$ give the heterobimetallic complexes $[TlM_4(\mu\text{-}pyS_2)_2(cod)_4][PF_6]$. An outstanding change in the coordination modes of the bridging ligands occurs on the incorporation of the Tl atom into the tetranuclear complexes with the concomitant formation of two unprecedented Tl−Rh bonds. The X-ray structure of the cation $[TlRh_4(\mu\text{-}pyS_2)_2(cod)_4]^+$ (**3**$^+$) shows an almost linear Rh−Tl−Rh bonded subunit with Tl−Rh separations of 2.7686(9) and 2.7706(9) Å. An unusual sawhorse coordination environment of the thallium atom is completed by binding to two pyridine nitrogen atoms. Theoretical calculations on this Rh−Tl interaction also support the formation of Rh−Tl bonds, which is accompanied by a slight electron transfer from thallium to both "Rh(cod)" fragments. An additional partial oxidation of the thallium center agrees with the large shift low field of the resonance (observed at 2926 ppm) in the $^{205}Tl\{^1H\}$ NMR spectrum of $[TlRh_4(\mu\text{-}pyS_2)_2(cod)_4][PF_6]$ (**3**) at 273 K. Moreover, complex **3** undergoes two irreversible one-electron anodic processes at 0.52 and 0.93 V ($CH_2Cl_2$, 0.1 V $s^{-1}$). These waves are shifted to higher potential than those of the parent complex $[Rh_4(\mu\text{-}pyS_2)_2(cod)_4]$. In addition, the cathodic response of this complex shows an irreversible reduction process at −1.48 V in which the $Tl^+$ ion is extruded. Interestingly, upon excitation in the solid state at 77 K, complex **3** shows strong luminescence which can be related to the Rh−Tl−Rh chromophore.

## Introduction

Considerable interest has been devoted to the design of molecules that provide efficient three-dimensional structures for the selective binding of metal atoms or ions.[1] Recent advances on host−guest chemistry remain focused on molecular recognition agents based on organic structures.[2] However, the search for inorganic analogues has become an area of increasing interest, and some inorganic cages,[3] metallocrowns,[4] metallomacrocycles,[5] or cluster cryptate complexes[6] have been recently developed. Metallomacrocages provide a unique opportunity for a selective encapsulation of ions directed by the formation of metal−metal bonds. This possibility, inaccessible with the purely organic counterparts, is particularly attractive with regard to the selective immobilization of toxic heavy metals such as beryllium, cadmium, mercury, thallium, or lead.[7]

Although evidence has recently been accumulated for bonding interactions between closed-shell ions (i.e. $d^{10}-d$,[10] $s^2-d^8$, and $s^2-d^{10}$), complexes containing thallium−transition metal bonds, particularly with Tl(I), are scarce.[8] As far as the $d^8$ transition

(1) (a) Slone, R. V.; Benkstein, K. D.; Bèlanger, S.; Hupp, J. T.; Guzei, I. A.; Rheingold, A. L. *Coord. Chem. Rev.* **1998**, *171*, 221. (b) Lehn, J.-M. *Supramolecular Chemistry. Concepts and Perspectives*; VCH: Weinhein, 1995. (c) Dietrich, B.; Viout, P.; Lehn, J.-M. *Macrocyclic Chemistry, Aspects of Organic and Inorganic Supramolecular Chemistry*; VCH: New York, 1993.

(2) (a) Nelson, I.; Mckee, V.; Morgan, G. *Progr. Inorg. Chem.* **1998**, *47*, 167. (b) Takemura, H.; Shinmyozu, T.; Inazu, T. *Coord. Chem. Rev.* **1996**, *156*, 183. (c) Roundhill, D. M. *Progr. Inorg. Chem.* **1995**, *43*, 533. (d) *Perspectives in Coordination Chemistry*; Williams, A. F., Floriani, C., Merbach, A. E., Eds.; VCH: Basel, 1992.

(3) (a) Allan, R. E.; Bashall, A.; Palmer, J. S.; McPartlin, M.; Mosquera, M. E. G.; Rawson, J. M.; Wheatley, A. E. H.; Wright, D. S. *Chem. Commun.* **1997**, 1975. (b) Lah, M. S.; Gibney, B. R.; Tierney, D. L.; Penner-Hahn, J. E.; Pecorato, V. L. *J. Am. Chem. Soc.* **1993**, *115*, 5857. (c) Huang, S.-P.; Kanatzidis, M. G. *Angew. Chem., Int. Ed. Engl.* **1992**, *31*, 787. (d) Müller, A.; Hovemeier, K.; Rohlfing, R. *Angew. Chem., Int. Ed. Engl.* **1992**, *31*, 1192. (e) Reuter, H. *Angew. Chem., Int. Ed. Engl.* **1992**, *31*, 1185.

(4) Pecoraro, V. L.; Stemmler, A. J.; Gibney, B. R.; Bodwin, J. J.; Wang, H.; Kampf, J. W.; Barwinski, A. *Progr. Inorg. Chem.* **1997**, *45*, 83.

(5) (a) Balch, A. L. *Progr. Inorg. Chem.* **1994**, *41*, 239. (b) Hiraki, K.; Khono, S.; Onishi, M.; Kuwahara, T.; Michita, Y. *Inorg. Chim. Acta* **1996**, *245*, 243. (c) Van Veggel, F. C. J. M.; Verboom, W.; Reinhoudt, D. N. *Chem. Rev.* **1994**, *94*, 279. (d) Ciriano, M. A.; Pérez-Torrente, J. J.; Oro, L. A.; Tiripicchio, A.; Tiripicchio-Camellini, M. *J. Chem. Soc., Dalton Trans.* **1991**, 225. (e) Ciriano, M. A.; Pérez-Torrente, J. J.; Viguri, F.; Lahoz, F. J.; Oro, L. A.;. Tiripicchio, A.; Tiripicchio-Camellini, M. *J. Chem. Soc., Dalton Trans.* **1990**, 1493. (f) Balch, A. L. *Pure Appl. Chem.* **1988**, *60*, 555.

(6) (a) Comstock, M. C.; Prussak-Wieckowska, T.; Wilson, S. R.; Shapley, J. R. *Organometallics* **1997**, *16*, 4033. (b) Hao, L.; Xiao, J.; Vittal, J. J.; Puddephatt, R. J.; Manojlovic-Muir, L.; Muir, K. W.; Tobari, A. A. *Inorg. Chem.* **1996**, *35*, 658. (c) Hao, L.; Vittal, J. J.; Puddephatt, R. J. *Organometallics* **1996**, *15*, 3115. (d) Ezomo, E. J.; Mingos, M. P.; Williams, I. D.; *J. Chem. Soc.; Chem. Commun.* **1987**, 924.

(7) (a) Yordanov, A. T.; Roundhill, D. M. *Coord. Chem. Rev.* **1998**, *170*, 93. (b) Stemmler, A. J.; Kampf, J. W.; Pecoraro, V. L. *Angew. Chem., Int. Ed. Engl.* **1996**, *35*, 2841. (c) Chinea, E.; Dominguez, X.; Mederos, A.; Brito, F.; Arrieta, J. M.; Sánchez, A.; Germain, G. *Inorg. Chem.* **1995**, *34*, 1579. (d) Cecconi, F.; Ghilardi, C. A.; Midollini, S.; Orlandini, A.; Vacca, A. *J. Organomet. Chem.* **1996**, *510*, 153. (e) Rupprecht, S.; Franklin, S. J.; Raymond, K. N. *Inorg. Chim. Acta* **1995**, *235*, 185. (f) Kahwa, I. A.; Miller, D.; Mitchel, M.; Fronczek, F. R.; Goodrich, R. G.; Williams, D. J.; O'Mahoney, C. A.; Slawin, A. M. Z.; Ley, S. V.; Groombridge, C. J. *Inorg. Chem.* **1992**, *31*, 3963.

(8) (a) Pyykkö, P. *Chem. Rev.* **1997**, *97*, 597. (b) Pyykkö, P. *Chem. Rev.* **1988**, *88*, 563.

10.1021/ic980988m CCC: $18.00 
Published on Web 04/28/1999

metal ions are concerned, significant bonding interactions ($s^2-d^8$) are observed in complexes containing metal ions from the third row of the transition series, mainly Pt(II)[6b−d,9,10] and Ir(I),[6a,11,12] where relativistic effects are believed to contribute significantly to bonding. However, regarding the counterparts with metal ions from the second row, only a few examples of Pd(II)−Tl(I) bonds have appeared in the literature.[13] On the other hand, it is well-known that compounds containing short metal−metal distances between relativistic heavy atoms such as Au, Pt, Tl, Pb have been shown to display luminescent properties.[14]

We have recently described the straightforward synthesis of homotetranuclear complexes $[M_4(\mu\text{-}pyS_2)_2(cod)_4]$ (M = Rh **1** or Ir **2**; cod = 1,5-cyclooctadiene), where two 2,6-pyridinedithiolate ($pyS_2$) ligands hold up four $d^8$ metallic centers arranged in a zigzag chain disposition.[15] A preliminary test showed residual nucleophilic character on the external sulfur atoms of the tetranuclear framework and prompted us to study the reactivity of these complexes toward metal cations. We report herein the synthesis and full characterization of new cationic pentanuclear heterobimetallic species which result from the encapsulation of Tl(I) into the tetranuclear structure. A theoretical study of the electronic structure with special regard to the intermetallic Rh−Tl bonding system is also discussed.

## Results and Discussion

**Synthesis.** Reaction of $[Rh_4(\mu\text{-}pyS_2)_2(cod)_4]$ (**1**) with an equimolar amount of $TlPF_6$ in dichloromethane−acetone gives the heterobimetallic complex $[TlRh_4(\mu\text{-}pyS_2)_2(cod)_4][PF_6]$ (**3**) immediately. The related compound $[TlIr_4(\mu\text{-}pyS_2)_2(cod)_4][PF_6]$ (**4**) is similarly obtained by reaction of $[Ir_4(\mu\text{-}pyS_2)_2(cod)_4]$ (**2**) with $TlPF_6$. However, the tetranuclear complexes $[M_4(\mu\text{-}pyS_2)_2(tfbb)_4]$ (M = Rh or Ir, tfbb = tetrafluorobenzobarrelene), containing a diolefin with a stronger $\pi$-acceptor character than cod, fail to react with thallium(I) salts. The incorporation of Tl(I) into the tetranuclear complexes was established in the first instance by the mass spectra, where both molecular ions (100%)—with the correct isotopic distribution at *m*/*z* 1331 and 1689, respectively—were observed. Both complexes are 1:1 electrolytes in acetone and exhibit two strong characteristic absorptions in the IR spectra corresponding to uncoordinated $PF_6^-$ anions. The structure of **3** has been determined by X-ray diffraction methods and a molecular diagram of the cation ($\mathbf{3}^+$) is shown as Figure 1. Table 1 displays selected bond distances and angles for $\mathbf{3}^+$.

It is noticeable that no reaction of **1** or **2** with $Pb^{2+}$, as $Pb(NO_3)_2$, an ion isoelectronic with $Tl^+$, has been observed. However, both complexes react with $d^{10}$ ions, such as $Ag^+$ and $Au^+$, to give insoluble products which are currently under further investigation. Compound $[TlRh_4(\mu\text{-}pyS_2)_2(cod)_4][PF_6]$ (**3**) is stable in refluxing THF or acetone solutions but decomposes in the presence of a slight excess of LiCl in a dichloromethane−methanol mixture (2:1) with elimination of the $Tl^+$ ion as TlCl. Interestingly, the parent complex **1** can be recovered quantitatively after removal of the insoluble thallium salt by filtration.

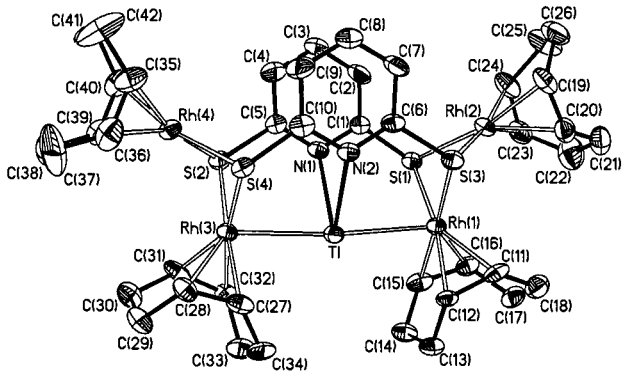


**Figure 1.** Molecular structure of the cation $[TlRh_4(\mu\text{-}pyS_2)_2(cod)_4]^+$ ($\mathbf{3}^+$), showing the atom numbering scheme used.

**Table 1.** Selected Bond Lengths (Å) and Angles[a] (deg) for $\mathbf{3}^+$

| | | | |
|---|---|---|---|
| Tl−Rh(1) | 2.7686(9) | Tl−Rh(3) | 2.7706(9) |
| Tl−N(1) | 2.611(7) | Tl−N(2) | 2.605(7) |
| Rh(1)−S(1) | 2.381(2) | Rh(3)−S(2) | 2.370(2) |
| Rh(1)−S(3) | 2.373(2) | Rh(3)−S(4) | 2.371(2) |
| Rh(2)−S(1) | 2.390(2) | Rh(4)−S(2) | 2.387(3) |
| Rh(2)−S(3) | 2.387(3) | Rh(4)−S(4) | 2.382(2) |
| S(1)−C(1) | 1.780(9) | S(2)−C(5) | 1.789(9) |
| S(3)−C(6) | 1.788(10) | S(4)−C(10) | 1.780(10) |
| Rh(1)−Tl−Rh(3) | 174.72(2) | N(1)−Tl−N(2) | 71.1(2) |
| Rh(1)−Tl−N(1) | 88.48(17) | Rh(3)−Tl−N(1) | 87.34(17) |
| Rh(1)−Tl−N(2) | 87.54(17) | Rh(3)−Tl−N(2) | 88.06(17) |
| Tl−Rh(1)−S(1) | 88.75(6) | Tl−Rh(3)−S(2) | 89.83(6) |
| Tl−Rh(1)−S(3) | 89.68(7) | Tl−Rh(3)−S(4) | 89.11(6) |
| Tl−Rh(1)−M(1) | 100.6(3) | Tl−Rh(3)−M(5) | 105.2(3) |
| Tl−Rh(1)−M(2) | 106.3(3) | Tl−Rh(3)−M(6) | 101.0(3) |
| S(1)−Rh(1)−S(3) | 87.40(8) | S(2)−Rh(3)−S(4) | 87.24(8) |
| S(1)−Rh(1)−M(1) | 170.6(3) | S(2)−Rh(3)−M(5) | 164.9(3) |
| S(1)−Rh(1)−M(2) | 91.1(3) | S(2)−Rh(3)−M(6) | 92.9(3) |
| S(3)−Rh(1)−M(1) | 92.6(3) | S(4)−Rh(3)−M(5) | 91.1(3) |
| S(3)−Rh(1)−M(2) | 163.9(3) | S(4)−Rh(3)−M(6) | 169.9(3) |
| M(1)−Rh(1)−M(2) | 86.3(4) | M(5)−Rh(3)−M(6) | 86.2(4) |
| S(1)−Rh(2)−S(3) | 86.88(9) | S(2)−Rh(4)−S(4) | 87.24(8) |
| S(1)−Rh(2)−M(3) | 172.8(3) | S(2)−Rh(4)−M(7) | 175.3(3) |
| S(1)−Rh(2)−M(4) | 93.1(3) | S(2)−Rh(4)−M(8) | 92.4(3) |
| S(3)−Rh(2)−M(3) | 91.5(3) | S(4)−Rh(4)−M(7) | 93.2(3) |
| S(3)−Rh(2)−M(4) | 173.7(3) | S(4)−Rh(4)−M(8) | 173.5(3) |
| M(3)−Rh(2)−M(4) | 87.7(5) | M(7)−Rh(4)−M(8) | 87.3(5) |

[a] M(1) to M(8) correspond to the midpoints of the olefinic bonds C(11)−C(12), C(15)−C(16), C(19)−C(20), C(23)−C(24), C(27)−C(28), C(31)−C(32), C(35)−C(36), and C(39)−C(40), respectively.

**Crystal and Molecular Structure of $[TlRh_4(\mu\text{-}pyS_2)_2(cod)_4][PF_6]$ (3).** The cation consists of a boat-shaped pentametallic chain supported by two 2,6-pyridinedithiolate groups acting as *S*,*N*,*S*′-tridentate ligands and showing a noncrystallographic approximate $C_{2v}$ symmetry. The 2,6-pyridinedithiolate ligands are bonded to the four rhodium atoms exclusively through the sulfur atoms, which coordinate in a $\mu_2$-fashion, i.e., as thiolate ligands. Each rhodium center is linked to two sulfur atoms of the two bridging ligands and to a 1,5-cyclooctadiene molecule chelating through the two olefinic bonds, resulting in a square planar environment for the external metal atoms, Rh(2) and Rh(4). Interestingly, Rh(1) and Rh(3) are also bonded to the

(9) Usón, R.; Forniés, J.; Tomás, M.; Garde, R. *J. Am. Chem. Soc.* **1995**, *117*, 1837.
(10) (a) Usón, R.; Forniés, J.; Tomás, M.; Garde, R.; Merino, R. *Inorg. Chem.* **1997**, *36*, 1383. (b) Ara, I.; Berenguer, J. R.; Forniés, J.; Gómez, J.; Lalinde, E.; Merino, R. I. *Inorg. Chem.* **1997**, *36*, 6461. (c) Renn, O.; Lippert, B.; Mutikainen, I. *Inorg. Chim. Acta* **1993**, *208*, 219. (d) Renn, O.; Lippert, B.; Mutikainen, I. *Inorg. Chim. Acta* **1993**, *208*, 219. (e) Balch, A. L.; Rowley, S. P. *J. Am. Chem. Soc.* **1990**, *112*, 6139. (f) Nagle, J. K.; Balch, A. L.; Olmstead, M. M. *J. Am. Chem. Soc.* **1988**, *110*, 319.
(11) Balch, A. L.; Nagle, J. K.; Olmstead, M. M.; Reedy, P. E., Jr. *J. Am. Chem. Soc.* **1987**, *109*, 4123.
(12) Balch, A. L.; Neve, F.; Olmstead, M. M. *J. Am. Chem. Soc.* **1991**, *113*, 2995.
(13) Balch, A. L.; Davis, B. J.; Fung, E. Y.; Olmstead, M. M. *Inorg. Chim. Acta* **1993**, *212*, 149.
(14) Lees, A. J. *Chem. Rev.* **1987**, *87*, 711.
(15) Pérez-Torrente, J. J.; Casado, M. A.; Ciriano, M. A.; Lahoz, F. J.; Oro, L. A. *Inorg. Chem.* **1996**, *35*, 1782.

central thallium atom, resulting in square pyramidal geometries for both internal rhodium atoms with the thallium center as a shared apex. The two pyramidal basal planes are nearly parallel (dihedral angle of 23.1(2)°) and, significantly, both rhodium atoms are shifted from the their basal planes toward the thallium center (0.2377(8) and 0.2422(7) Å for Rh(1) and Rh(3), respectively). The geometry of the central metal framework subunit (Rh−Tl−Rh) is very similar to that found in the anionic complex $[Tl\{Pt(C_6F_5)_4\}_2]^{2-}$, where two pyramidal platinum environments share a common thallium apex (Pt−Tl−Pt 179-(1)°).[9] Furthermore, the thallium center in $\mathbf{3}^+$ is also found within bonding distance of the two pyridine nitrogen atoms, resulting in an anomalous sawhorse coordination environment.

The two 2,6-pyridinedithiolate ligands are roughly planar and nearly parallel with a dihedral angle between the two pyridine rings of 14.0(3)°. The sulfur atoms, S(1)−S(4), show deviations from these ring planes in the range 0.130−0.197(3) Å, in all cases toward the outer side of the pocket framework defined by the two $pyS_2$ bridging ligands. The exocyclic C−S distances of 1.78(1) Å, are rather longer than in the parent complex **1** and comparable to those for a single C−S bond, evidence of the lack of electron delocalization of the lone pair on the sulfurs into the aromatic ring and the thiolate character of these sulfur atoms.

The distances between the external and internal rhodium atoms [Rh(2)−Rh(1) 2.9272 and Rh(4)−Rh(3) 2.9364(11) Å] are characteristic of intermetallic interactions in dimers of square planar $d^8$ complexes.[16a] However, in **3** these short contacts seem to be nonattractive since the external rhodium atoms lie 0.1293 and 0.1071(7) Å out of their respective coordination planes outward from the inner rhodium atoms. This observation contrasts with the usual deviation from square planar coordination of the Rh(I) atoms toward the second metal atom found in $[Rh_2(\mu\text{-}L)_2(\text{diolefin})_2]$ complexes.[16b,c] The dihedral angles between the coordination planes of the external and internal rhodium atoms are large, 103.7 and 104.9(2)°, respectively, and are a consequence of the open-book structure imposed by the $\mu_2$-coordination mode of the thiolato moieties.

The most important feature of the structure of $\mathbf{3}^+$ is the coordination environment of the thallium atom. While, as commented above, there is clear evidence of thallium(I)−rhodium bonding, the relatively long Tl−N separation points to a weak nitrogen coordination. The Tl−Rh(1) and Tl−Rh(3) distances, 2.7686(9) and 2.7706(9) Å, respectively, are well below the sum of the metallic radii (3.04 Å)[17] and are significantly shorter than the Tl−Ir distances found in the compound $[Ir_2Tl(CO)_2Cl_2\{\mu\text{-}(Ph_2PCH_2)_2AsPh\}_2]$, 2.958 and 2.979(1) Å, where Tl−Ir metal−metal bonds have been reported.[11] Additional theoretical calculations on this Rh−Tl interaction also support the existence of Rh−Tl bonds (see below). The Rh−Tl−Rh bonding subunit is almost linear, 174.72(2)°; however, it is important to note that the deviation from linearity is not toward the frequent Tl(I) tetrahedral geometry, since the thallium atom is 0.1276(6) Å away from the vector Rh(1)−Rh(3) in a direction opposite to the nitrogen atoms. Despite this unusual coordination geometry, the observed Tl−N distances, 2.611 and 2.605(7) Å, support the coordination of the pyridine nitrogen atoms to the thallium center: similar distances have been found in the related anionic complexes[18] $[(bipy)Tl\{Fe(CO)_4\}_2]^-$ and $[(phen)Tl\{Fe(CO)_4\}_2]^-$, 2.61(1) and 2.58(1) Å, respectively, where the thallium environment is closely related to that found in $\mathbf{3}^+$, or in neutral thallium(I) tris-(pyrazolyl)borate complexes of the type $[Tl(PzR_2)_3BH]$ (Tl−N distances in the range 2.498−2.724 Å).[19] Nevertheless, the $sp^2$ nitrogen lone pair orientation, which is directed approximately 30° away from the thallium center, suggests the existence of some degree of electrostatic contribution in the Tl−N bonds.

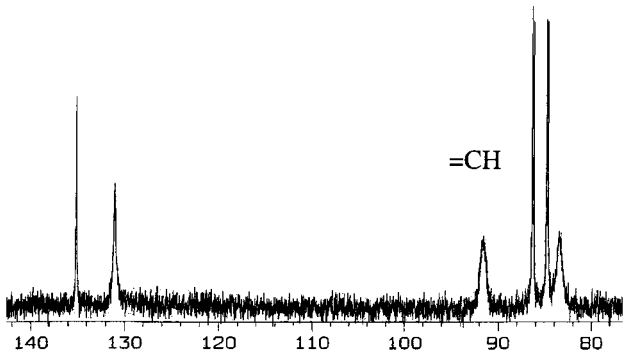


**Figure 2.** Aromatic and olefinic regions of the $^{13}C\{^1H\}$ NMR spectrum of $[TlRh_4(\mu\text{-}pyS_2)_2(cod)_4][PF_6]$ (**3**) in $CD_2Cl_2$ at 293 K.

Strong metal−metal bonds involving heavier transition elements (mostly platinum and iridium) and main group ions with an $s^2$ electronic configuration have been observed through structural and spectroscopic studies.[8a] However, the complex $[TlRh_4(\mu\text{-}pyS_2)_2(cod)_4][PF_6]$ (**3**) has no precedent since no related examples showing Tl−Rh bonds have been structurally characterized. Nevertheless, very recently some heterometallic porphirinate dimers containing a ligand-unsupported rhodium−thallium metal−metal bond of formula [(porph)Tl−Rh(porph′)] (porph and porph′ = octaethylporphyrin dianion or tetraphenylporphyrin dianion) have been characterized by multinuclear NMR spectroscopy.[20]

**NMR Spectroscopy ($^1$H, $^{13}$C, and $^{205}$Tl).** The available spectroscopic information for the cations $\mathbf{3}^+$ and $\mathbf{4}^+$ is in agreement with the structure found in the solid state for **3** since a $C_{2v}$ symmetry is detected for the bridging ligands in both the $^1H$ and $^{13}C\{^1H\}$ NMR spectra. In addition, a fluxional process operating even at 213 K produces the broadening of two resonances from the olefinic cod carbons while the other two are very sharp in the $^{13}C\{^1H\}$ NMR spectrum of **3** (Figure 2). The static cod ligands should be those coordinated to the rhodium atoms bonded to thallium, while the dynamic process should affect the two external "Rh(cod)" fragments. This interpretation is in accordance with the fluxionality observed in doubly thiolate-bridged dinuclear complexes having diolefin as ancillary ligands[21] and accounts for the lack of the C−S resonance and the slight broadening of the two observed resonances from the remaining carbon atoms of the 2,6-pyridinedithiolate ligands in the $^{13}C\{^1H\}$ NMR spectra at 213 K.

(16) (a) Aullón, G.; Alvarez, S. *Chem. Eur. J.* **1997**, *3*, 655, and references therein. (b) Tiripicchio, A.; Tiripicchio-Camellini, M.; Usón, R.; Oro, L. A.; Ciriano, M. A.; Viguri, F., *J. Chem. Soc., Dalton Trans.* **1984**, 125. (c) Lahoz, F. J.; Viguri, F.; Ciriano, M. A.; Oro, L. A.; Foces-Foces, C.; Cano, F. H. *Inorg. Chim. Acta* **1987**, *128*, 119.

(17) Greenwood, N. N.; Earnshaw, A. *Chemistry of the Elements*, 2nd ed.; Butterworth Heinemann: Oxford, U.K., 1997.

(18) Cassidy, J. M.; Whitmire, K. H. *Inorg. Chem.* **1989**, *28*, 1435.

(19) (a) Amoroso, A. J.; Jeffery, J. C.; Jones, P. L.; McCleverty, J. A.; Psillakis, E.; Ward, M. D. *J. Chem. Soc., Chem. Commun.* **1995**, 1175. (b) Yoon, K.; Parkin, G. *Polyhedron* **1995**, *14*, 811. (c) Renn, O.; Venanzi, L. M.; Marteletti, A.; Gramlich, V. *Helv. Chim. Acta* **1995**, *78*, 993.

(20) (a) Daphnomili, D.; Scheidt, W. R.; Zajicek, J.; Coutsolelos, A. G. *Inorg. Chem.* **1998**, *37*, 3675. (b) Coutsolelos, A. G.; Daphnomili, D. *Inorg. Chem.* **1997**, *36*, 4614.

(21) (a) Ciriano, M. A.; Pérez-Torrente, J. J.; Lahoz, F. J.; Oro, L. A. *J. Chem. Soc., Dalton Trans.* **1992**, 1831. (b) Abel, E. W.; Orrel, K. G. *Progr. Inorg. Chem.* **1994**, *32*, 1.

Proton-decoupled $^{205}$Tl NMR spectroscopic studies performed on organothallium and inorganic thallium compounds have shown that the thallium chemical shift range is very sensitive both to the oxidation state and to the coordination number of the metal. However, surprisingly few metal−thallium compounds have been studied by $^{205}$Tl NMR spectroscopy, although $^{205}$Tl nucleus is the third most receptive spin-$^1/_2$ nuclide.[22] The thallium atom in **3** is observed as a broad featureless resonance at 2926 ppm in the $^{205}$Tl{$^1$H} NMR spectrum at 273 K in $CD_2Cl_2$; the large line width ($w_{1/2}$ = 950 Hz) is in agreement with the coordination of quadrupolar N atoms of the 2,6-pyridinedithiolate ligands to thallium. The signal is shifted to 2883 ppm at 175 K, but no significant sharpening is observed, as expected from a quadrupolar relaxation mechanism.[23]

The spin−spin coupling constants involving the thallium nucleus are generally large.[24] In fact, $^{103}$Rh−$^{205}$Tl spin−spin coupling constants ranging from 5100 to 5300 Hz have recently been observed in heterometallic porphirinate dimers [(porph)Tl−Rh(porph′)].[20a] Bearing in mind the shape of the resonance, a small coupling to the rhodium atoms ($J \leq 500$ Hz) cannot be excluded, although the weak s-character[25] and the largely ionic nature (electrostatic contribution) of the Tl−Rh bonds could also be reasonable explanations for the lack of an observable $^{103}$Rh−$^{205}$Tl spin−spin coupling.

As far as the thallium chemical shift is concerned, it is well-known that the resonance frequency of thallium in the +1 oxidation state is normally lower than that of thallium in the +3 oxidation state.[26] However, the observed chemical shift in the $^{205}$Tl NMR spectrum for compound **3** lies far outside the typical −200 to 200 ppm range for Tl(I) and falls into the expected range for Tl(III) compounds: 2000 to 3000 ppm.[27] Although the oxidation state of the metal is not the only factor to determine the chemical shift, the greatly shifted low-field resonance is in accordance with theoretical studies (see below) that suggest a high positive charge on the thallium center. However, significantly downfield chemical shifts have been observed for a Ru−Tl(I) complex[28] and, interestingly, for some thallium−iron carbonyl compounds,[29] where the Tl(I) center exhibits a four-coordinate environment closely related to that found in **3**. In particular, chemical shifts ranging between 4400 and 5800 ppm are observed for the complexes [(L−L)Tl{Fe(CO)$_4$}$_2$]$^-$ (L−L = bipy, en, phen, tmda). This observation can be rationalized in terms of the spin−orbit effects on the chemical shift of the thallium nucleus induced by the bonding to heavy atoms such as iron or rhodium. In the case of p-block main group central atoms in low oxidation states, significant deshielding is expected when bonded to heavy atoms with bonds involving very little s character.[30]

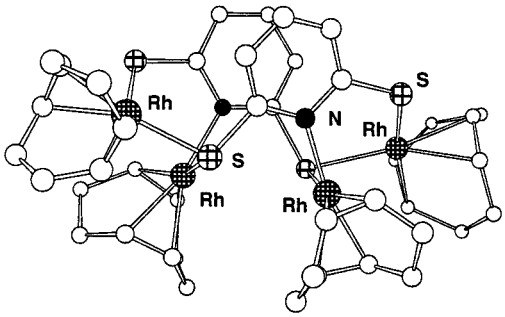


**Figure 3.** Chem3D representation of the molecular structure of [Rh$_4$($\mu$-pyS$_2$)$_2$(cod)$_4$] (**1**).

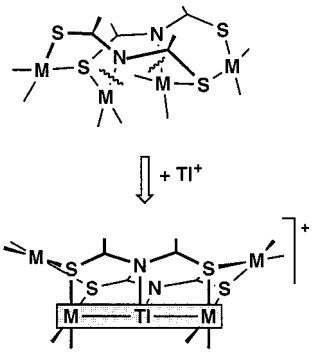


**Figure 4.** Framework reorganization leading to the encapsulation of $Tl^+$ into the [M$_4$($\mu$-pyS$_2$)$_2$(cod)$_4$] tetranuclear structures.

**Structure and Bonding.** From a structural point of view, **3**$^+$ can be envisaged as the result of the coordination of the [(cod)Rh−Tl−Rh(cod)]$^{3+}$ moiety to the 12-membered metallomacrocycle [Rh$_2$($\mu$-pyS$_2$)$_2$]$^{2-}$ containing sulfur and nitrogen atoms as binding sites. Taking into account the structure of precursor **1** (Figure 3), the formation of **3** could be envisaged as a structural reorganization process involving the breaking of the Rh−N bonds and the formation of new Rh−S and Tl−N bonds (Figure 4). In such a manner, the molecular framework provides the proper spatial requirements to accommodate the Tl(I) atom, and the Rh−Tl and Rh−N bonds provide the necessary energetic stabilization for the formation of **3**. Since the d$^8$ metal ions can be regarded as closed-shell ions, the bonding system Rh(I)−Tl(I)−Rh(I) corresponds to a d$^8$−s$^2$−d$^8$ combination involving closed-shell metals. This and related closed-shell interactions have been studied theoretically using different approaches, ranging from extended Hückel formalism to DFT calculations, and have recently been reviewed by Pyykkö.[8a] This type of bonding interaction has been attributed to correlation effects, although no negligible ionic contribution has been proposed is some cases. In addition, the expected relativistic effects for heavy elements strengthen the closed-shell attraction, but only to a moderate extent.

This theoretical interpretation can be understood in terms of the "*metallophilic attraction*" between closed-shell metals[31] and it is also applicable to explain the Tl−Rh bonds in the cation **3**$^+$. The term "*aurophilicity*" was originally coined to describe intra- and intermolecular Au(I)−Au(I) interactions; however, it soon became clear that analogous metallophilic effects could also involve metal atoms other than gold, such as Tl(I) and Hg(II).[8a] Although the Au(I)−Au(I) interaction is among the strongest closed-shell interactions, the search for metallophilic

(22) Mann, B. E. *NMR of Newly Accessible Nuclei*; Laszlo, P., Ed.; Academic Press: New York, 1983; Vol 2.
(23) Roe, D. C. *Experimental Organometallic Chemistry*; Wyda, A. L., Darensbourg, M. Y., Eds.; American Chemical Society: Washington, DC, 1987; Vol. 357.
(24) (a) Hinton, J. F. *Magn. Res. Chem.* **1987**, *25*, 659. (b) Hinton, J. F.; Metz, K. R.; Briggs, R. W. *Annual Reports on NMR Spectroscopy*; Webb, G. A., Ed.; Academic Press: London, 1982; Vol. 13.
(25) Berg, K. E.; Glaser, J.; Read, M. C.; Tóth, I. *J. Am. Chem. Soc.* **1995**, *117*, 7550.
(26) Janiak, C. *Coor. Chem. Rev.* **1997**, *163*, 107.
(27) (a) Berg, K. E.; Blixt, J.; Glaser, J. *Inorg. Chem.* **1996**, *35*, 7074. (b) Hinton, J. F.; Metz, K. R.; Briggs, R. W. *Progr. NMR Spectrosc.* **1988**, *20*, 423. (c) Glaser, J. *Advances in Inorganic Chemistry*; Sykes, G., Ed.; Academic Press: San Diego, CA, 1995; Vol. 43, p 1.
(28) Bianchini, C.; Masi, D.; Linn, K.; Mealli, C.; Peruzzini, M.; Zanobini, F. *Inorg. Chem.* **1992**, *31*, 4036.
(29) van Hal, J. W.; Alemany, L. B.; Whitmire, K. H. *Inorg. Chem.* **1997**, *36*, 3152.
(30) (a) Kaupp, M.; Malkina, O. L.; Malkin, V. G.; Pyykkö, P. *Chem. Eur. J.* **1998**, *4*, 118. (b) Edlund, U.; Lejon, T.; Pyykkö, P.; Venkatachalam, T. K.; Buncel, E. *J. Am. Chem. Soc.* **1987**, *109*, 5982.
(31) Pyykkö, P.; Li, J.; Runeberg, N. *Chem. Phys. Lett.* **1994**, *218*, 133.

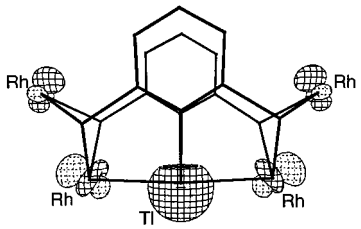


**Figure 5.** Drawing of the HOMO in $\mathbf{3}^+$ showing the intermetallic antibonding character; the cod ligands have been excluded for clarity.

effects involving lighter metal atoms is of considerable current interest.[32] To assess the extent to which the Rh−Tl bonds contribute to the stabilization of the structure an extended Hückel molecular orbital (EHMO) calculation was performed.[33]

If only the intermetallic bonding system is considered, the molecular orbital diagram for $\mathbf{3}^+$ results from the interaction between a filled set of molecular orbitals (including the HOMO, Figure 5) built up with rhodium $4d_{z^2}$ and thallium 6s atomic orbitals and an empty set assembled with the $p_z$ atomic orbitals of the three metal centers (*z* parallel to the Rh−Rh vector). At EHT level, mixing of these molecular orbitals results in an overall stabilization, thereby imparting stability to the Rh−Tl−Rh unit. This molecular orbital interpretation is analogous to that reported for the compound $[Ir_2Tl(CO)_2Cl_2\{\mu\text{-}Ph_2PCH_2\}_2\text{-}AsPh\}_2]$[11] containing a Ir−Tl−Ir bonded moiety; however, it is important to note the different geometry of the M($d^8$)−Tl(I)−M($d^8$) central unit since it is bent in the latter, 139.4(1)°, but is almost linear in $\mathbf{3}^+$: 174.72(2)°. Another closely related and structurally characterized M($d^8$)−Tl(I)−M($d^8$) system, *cis*-$[(NH_3)_2Pt(1\text{-}MeT)_2Tl(1\text{-}MeT)_2Pt(NH_3)_2]^+$ (1-MeT = 1-methylthymine anion), also exhibits a bent geometry (136.7(1)°), but in this case, a simplified approach—in terms of the stereoactivity of the $6s^2$ thallium *inert pair*—was used to explain the metal disposition.[10d] In this alternative explanation, the coordination environment of Tl(I) in $\mathbf{3}^+$ could also be interpreted in terms of the VSEPR theory since, formally, the thallium atom has five electron pairs in its valence shell, one lone pair (the 6s orbital) and four bonding pairs (one from each rhodium or nitrogen bonded atom), and the resulting geometry can be viewed as a distorted trigonal bipyramid. This ideal coordination would locate the nitrogen atoms together with the nonbonding lone pair in the equatorial plane and the two rhodiums at the apical positions. Under this approximation, the deformation of the ideally linear Rh−Tl−Rh moiety (away from the lone pair) is reasonable. A bent geometry, with greater Rh−Tl−Rh bond angle, as observed for the above-mentioned Pt−Tl or Ir−Tl complexes,[10d,11] is not favored in **3**, since lower values for the Rh−Tl−Rh angle would result in an elongation of the Tl−N distances and thus a weakening of the Tl−N bonds.

The formation of the Tl−Rh bonds is accompanied by a slight electron transfer from thallium to both "Rh(cod)" fragments, which leads to an additional partial oxidation of the thallium center. This is reflected in the high Mulliken positive charge calculated for the thallium atom (approximately 1.50 $e^-$) at the EHT level and agrees with the greatly shifted low-field resonance observed in the $^{205}$Tl NMR spectrum. This phenomenon has recently been observed by Glaser et al. in the heterodinuclear series $[(CN)_5Pt{-}Tl(CN)_{n-1}]^{(n-1)-}$ ($n$ = 1−4) containing unsupported Tl−Pt bonds where a donor−acceptor

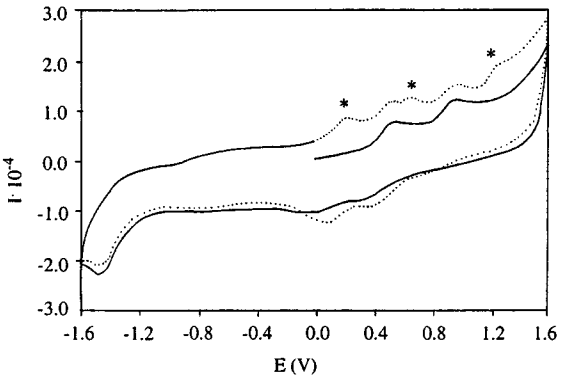


**Figure 6.** Cyclic voltammogram of $[TlRh_4(\mu\text{-}pyS_2)_2(cod)_4]^+$ ($\mathbf{3}^+$) in $CH_2Cl_2$ at 0.1 V $s^{-1}$: first cycle (solid line) and second cycle (dotted line). Asterisks show the one-electron anodic processes corresponding to the electrogenerated tetranuclear precursor $[Rh_4(\mu\text{-}pyS_2)_2(cod)_4]$ (**1**).

bonding model has also been proposed. The most pronounced electron transfer from platinum to thallium takes place in the absence of cyanide ligands coordinated to thallium ($n$ = 1), as detected by NMR spectroscopy, both in the thallium chemical shift and the $^1J_{Pt-Tl}$ spin−spin coupling.[34]

**Electrochemical Behavior.** The MO diagram also shows that the energy gap between the HOMO and LUMO is smaller than the energy difference between the HOMO and the next lowest energy MO. Bearing in mind the peculiar antibonding nature of the HOMO (Figure 5), removal of electrons from this orbital should result in an overall stabilization. In fact, $[TlRh_4(\mu\text{-}pyS_2)_2\text{-}(cod)_4]^+$ ($\mathbf{3}^+$) undergoes two irreversible one-electron anodic processes at 0.52 and 0.93 V ($CH_2Cl_2$, 0.1 V $s^{-1}$), probably associated with the formation of the corresponding di- and tricationic species (Figure 6). The parent complex $[Rh_4(\mu\text{-}pyS_2)_2\text{-}(cod)_4]$ (**1**) undergoes two reversible one-electron oxidation processes at formal electrode potentials of 0.16 and 0.58 V, respectively corresponding to the electrogeneration of the monocationic $[Rh_4(\mu\text{-}pyS_2)_2(cod)_4]^+$ and dicationic $[Rh_4(\mu\text{-}pyS_2)_2(cod)_4]^{2+}$ species, and an irreversible electron transfer at 1.21 V ($CH_2Cl_2$, 0.1 V $s^{-1}$).[15] Therefore, complex **3** is harder to oxidize than complex **1**. In addition, the cathodic response of complex **3** shows an irreversible one-electron reduction process at −1.48 V. Interestingly, scanning beyond the reduction potential results in the observation of three extra waves that agree with those corresponding to complex **1**. This observation suggests that the $Tl^+$ ion is extruded either in the reduction process of **3** or after the oxidation of the electrogenerated species following the reduction process.

**Electronic Properties.** A comparison of the electronic absorption spectra of complexes **3** and **4** with the parent tetranuclear complexes **1** and **2** also shows evidence of Rh−Tl and Ir−Tl bonds. The absorption spectrum of $[Rh_4(\mu\text{-}pyS_2)_2\text{-}(cod)_4]$ (**1**) exhibits two bands at 377 and 501 nm which have been assigned to MLCT and $d\sigma^* \rightarrow p\sigma$ transitions,[35] respectively. However, the absorption spectrum of **3** show both red-shifted absorptions at 430 and 509 nm and an intense absorption at 681 nm related to the presence of the thallium atom (Figure 7a). Similarly, a strong absorption at 854 nm is observed in the electronic spectrum of **4** apart from those at 484, 608, and 699

(32) Poblet, J.-M.; Bénard, M. *Chem. Commun.* **1998**, 1179.
(33) (a) Mealli, C.; Proserpio, D. M. *J. Chem. Educ.* **1990**, *67*, 399. (b) Hoffmann, R. *J. Chem. Phys.* **1963**, *39*, 1397. (c) Hoffmann, R.; Lipscomb, W. N. *J. Chem. Phys.* **1962**, *36*, 2179. (d) Hoffmann, R.; Lipscomb, W. N. *J. Chem. Phys.* **1962**, *36*, 2872.
(34) Maliarik, M.; Berg, K.; Glaser, J.; Sandström, M.; Tóth, I. *Inorg. Chem.* **1998**, *37*, 2910.
(35) (a) Yip, H. K.; Lin, H. M.; Che, Ch. M. *Inorg. Chem.* **1993**, *32*, 3402. (b) Rodman, G. S.; Daws, C. A.; Mann, K. R. *Inorg. Chem.* **1988**, *27*, 3347. (c) Balch, A. L.; Fosset, L. A.; Olmstead, M. M.; Reedy, P. E., Jr. *Organometallics* **1986**, *10*, 129.

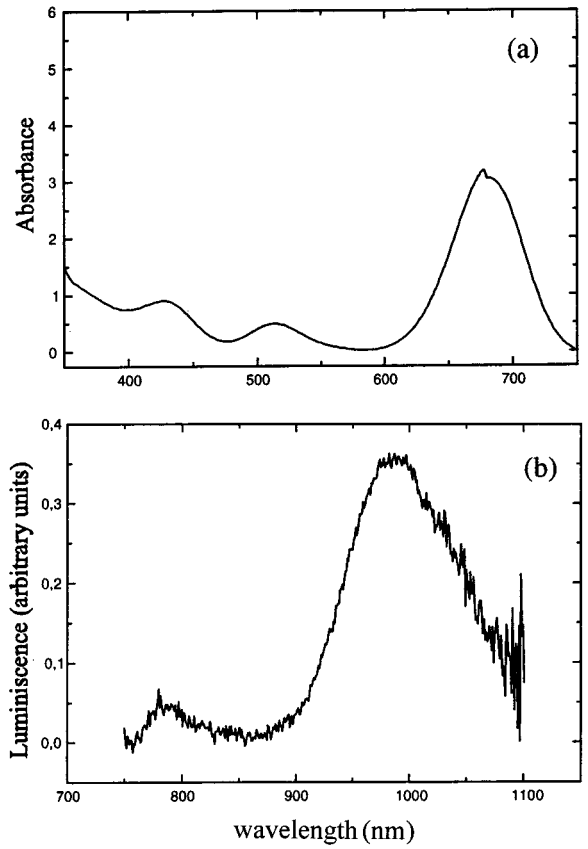


**Figure 7.** Electronic absorption spectrum of $[TlRh_4(\mu\text{-}pyS_2)_2(cod)_4][PF_6]$ (**3**) in dichloromethane solution at 298 K (a) and the luminescence spectrum of a solid sample upon excitation at 705 nm (b).

nm related to those observed for complex $[Ir_4(\mu\text{-}pyS_2)_2(cod)_4]$ (**2**) at 361, 452, and 564 nm.

It is noticeable that the electronic spectra of **1** is similar to those observed for related rhodium and iridium dinuclear complexes $[\{M(\mu\text{-}C_7H_4NS_2)(diolefin)\}_2]$, where only one $d\sigma^* \rightarrow p\sigma$ absorption is detected.[36] This fact is in agreement with the intermetallic interactions found in **1**, since only short intermetallic distances are found between the external rhodium atoms (3.1435(5) Å) but not between the rhodium atoms across the $C_2$ axis (Figure 3).[15] Thus, the homotetranuclear framework can be described as the assembling of two dinuclear units, and consequently only one $d\sigma^* \rightarrow p\sigma$ absorption is observed. However, the observation of two absorption maxima attributable to $d\sigma^* \rightarrow p\sigma$ excitations for the iridium tetranuclear complex **2** (452 and 564 nm) could be associated with the existence of deformational isomers, implying modifications in the Ir−Ir distances, as reported for the optical properties of 1,8-diisocyanomethane iridium dinuclear complexes.[37]

The iridium tetranuclear complex **2** is luminescent in the solid state, but no emission was detected for the rhodium tetranuclear complex **1**. The emission spectrum at room temperature (excitation at 600 nm) shows a broad band with a maximum at 810 nm (12 350 $cm^{-1}$) with a full width at half-maximum (fwhm) of 1940 $cm^{-1}$. At 77 K a narrow band at 800 nm (12 500 $cm^{-1}$) with a fwhm of 1460 $cm^{-1}$ is observed. However, solutions of **2** do not show luminescence, even at 77 K. The luminescent behavior of organometallic Ir(I) complexes is a well-known phenomenon, and the emission has been frequently ascribed to MLCT transitions.[14] Complex $[TlRh_4(\mu\text{-}pyS_2)_2(cod)_4][PF_6]$ (**3**) shows strong luminescence upon excitation in the solid state at 77 K that can be related to the Rh−Tl−Rh chromophore.[10a,38] The emission spectrum (excitation at 705 nm) displays a weak band with a maximun at 780 nm (12 820 $cm^{-1}$) and a intense band at 990 nm (10 100 $cm^{-1}$) with a fwhm of 1180 $cm^{-1}$ (Figure 7b). In contrast, the related iridium analogue $[TlIr_4(\mu\text{-}pyS_2)_2(cod)_4][PF_6]$ (**4**) does not exhibit luminescent properties, even at low temperature, probably due to a nonradiative return to the fundamental state.[39]

## Conclusions

The homotetranuclear rhodium and iridium complexes $[M_4(\mu\text{-}pyS_2)_2(cod)_4]$ behave as encapsulating agents for the thallium(I) ion through the formation of cationic pentametallic species. The Tl(I) encapsulation seems to be determined by subtle electronic factors and involves an important structural reorganization driven not only by the multiple coordination possibilities of the doubly deprotonated 2,6-dimercaptopyridine ligands but also by the existence of $d^8-s^2-d^8$ bonding interactions that contribute to the stabilization of the structure. In particular, the presence of the Rh−Tl bonds in compound $[TlRh_4(\mu\text{-}pyS_2)_2(cod)_4][PF_6]$ (**3**) is evidenced both by the X-ray crystal structure and optical properties. This interaction is supported by theoretical calculations, although it can also be understood in terms of the "*metallophilic attraction*" between closed-shell metal cations.

## Experimental Section

**General.** All manipulations were performed under an inert atmosphere (nitrogen or argon) using standard Schlenk techniques. Solvents were dried by known methods and distilled under nitrogen immediately prior to use. The tetranuclear complexes $[Rh_4(\mu\text{-}pyS_2)_2(cod)_4]$ and $[Ir_4(\mu\text{-}pyS_2)_2(cod)_4]$ were prepared directly from the corresponding $[\{M(\mu\text{-}OMe)(cod)\}_2]$ and 2,6-dimercaptopyridine $[py(SH)_2]$ as previously described.[15]

**Physical Measurements.** $^1H$ and $^{13}C\{^1H\}$ NMR spectra were recorded on a Varian Gemini 300 spectrometer operating at 300.08 and 75.46 MHz, respectively. Chemical shifts are reported in ppm and referenced to $SiMe_4$ using the residual signal of the deuterated solvent ($^1H$ and $^{13}C$). The proton-decoupled $^{205}Tl$ NMR spectrum was recorded on a AMX 300 BRUKER spectrometer operating at 173.63 MHz using a specific 10 mm thallium probe (Bruker). The different temperatures (298−175 K) were adjusted using the spectrometer temperature control unit. Data were obtained using a pulse of 23.9 $\mu$s corresponding to a 45° flip angle and referred to an aqueous solution of $TlNO_3$ ($2.0 \times 10^{-3}$ M).[24b] Chemical shifts are given in ppm toward higher frequency. The spectral region (−500/4000 ppm) was searched in regular increments using a spectral width setting of 35 kHz. IR spectra were recorded on a Nicolet 550 spectrometer using Nujol mulls between polyethylene sheets or in solution in a cell with NaCl windows. Elemental analyses were performed with a Perkin-Elmer 240-C microanalyzer. Conductivities were measured in ca. $5 \times 10^{-4}$ M dichloromethane solutions using a Philips PW 9501/01 conductimeter. Mass spectra were recorded in a VG Autospec double-focusing mass spectrometer operating in the $FAB^+$ mode. Ions were produced with the standard $Cs^+$ gun at ca. 30 kV; 3-nitrobenzyl alcohol (NBA) was used as matrix.

The optical absorption spectra were registered on a U-3400 Hitachi spectrophotometer in solution ($CH_2Cl_2$, $10^{-4}/10^{-5}$ M) or in solid state (KBr pellets), in the visible and near-UV ranges. Luminiscence spectra

(36) Ciriano, M. A.; Pérez-Torrente, J. J.; Oro, L. A.; Viguri, F.; Tiripicchio, A.; Tiripicchio-Camellini, M.; Lahoz, F. J. *J. Chem. Soc., Dalton Trans.* **1990**, 1493.

(37) Exstrom, C. L.; Britton, D.; Mann, K. R.; Hill, M. G.; Miskowski, V. M.; Schaefer, W. P.; Gray, H. B. *Inorg. Chem.* **1996**, *35*, 549.

(38) (a) Franciò, G.; Scopelliti, R.; Arena, G. C.; Bruno, G.; Drommi, D.; Faraone, F. *Organometallics* **1998**, *17*, 338. (b) Balch, A. L.; Neve, F.; Olmstead, M. M. *Inorg. Chem.* **1991**, *30*, 3395. (c) Wang, S.; Fackler, J. P., Jr.; King, C.; Wang, J. C. *J. Am. Chem. Soc.* **1988**, *110*, 3308.

(39) Blasse, G.; Grabmaier, B. C. *Luminescent Materials*; Springer-Verlag: Berlin, 1994.

were obtained using a standard calibrated tungsten−halogen lamp (1000 W) and corrected for the instrumental response of the equipment.

Cyclic voltammetric experiments were performed with an EG&G PARC Model 273 potentiostat/galvanostat. A three-electrode glass cell consisting of a platinum-disk working electrode, a platinum-wire auxiliary electrode, and a standard calomel reference electrode (SCE) was used. Tetra-*n*-butylammonium hexafluorophosphate (TBAH) was employed as supporting electrolyte. Electrochemical experiments were carried out under nitrogen in ca. $5 \times 10^{-4}$ M dichloromethane solutions of the complexes and 0.1 M in TBAH. The $[Fe(C_5H_5)_2]^+/[Fe(C_5H_5)_2]$ couple is observed at +0.47 V under these experimental conditions.

**Preparation of the Complexes. $[TlRh_4(\mu\text{-}pyS_2)_2(cod)_4][PF_6]$ (3).** $TlPF_6$ (0.031 g, 0.089 mmol) was added to a solution of $[Rh_4(\mu\text{-}pyS_2)_2(cod)_4]$ (**1**) (0.100 g, 0.089 mmol) in an acetone−dichloromethane mixture (2:1, 15 mL) to give a deep brown-green solution which was stirred for 2 h. Concentration of the solution under vacuum to 1 mL and addition of hexanes (5 mL) gave the complex as a brown microcrystalline solid which was filtered off, washed with hexanes, and dried under vacuum. Yield: 0.120 g (91%). Anal. Calcd for $C_{42}H_{54}F_6N_2PRh_4S_4Tl$: C, 34.17; H, 3.69; N, 1.90. Found: C, 34.08; H, 3.15; N, 1.89. MS (FAB+, $CH_2Cl_2$, *m*/*z*): 1331 ($TlRh_4(pyS_2)_2(cod)_4^+$, 100), 1126 ($Rh_4(pyS_2)_2(cod)_4^+$, 40). $\Lambda_M$ ($\Omega^{-1}$ cm$^2$ mol$^{-1}$): 128 (acetone, $4.99 \times 10^{-4}$ M). $^1$H NMR ($CD_2Cl_2$, 293 K) $\delta$: 7.15 (d, 4H, $J_{H-H}$ = 7.8 Hz), 6.76 (t, 2H, $J_{H-H}$ = 7.8 Hz) ($pyS_2$), 5.16 (m, 4H, =CH), 4.95 (m, 4H, =CH), 4.73 (m, 4H, =CH), 4.44 (m, 4H, =CH), 3.05 (m, 4H, >$CH_2$), 2.82−2.08 (m, 28H, >$CH_2$) (cod). $^{13}$C{$^1$H} NMR ($CD_2Cl_2$, 293 K) $\delta$: 135.1, 131.0 (br) ($pyS_2$), 91.5 (br), 86.2 (d, $^1J_{Rh-C}$ = 11.5 Hz), 84.7 (d, $^1J_{Rh-C}$ = 10.6 Hz), 83.5 (br) (=CH), 32.2, 32.0, 31.2 (>$CH_2$) (cod). $^{205}$Tl{$^1$H} NMR ($CD_2Cl_2$, 273 K): 2926.

**$[TlIr_4(\mu\text{-}pyS_2)_2(cod)_4][PF_6]$ (4).** $TlPF_6$ (0.023 g, 0.067 mmol) and $[Ir_4(\mu\text{-}pyS_2)_2(cod)_4]$ (**2**) (0.100 g, 0.067 mmol) were reacted in an acetone−dichloromethane mixture (2:1, 15 mL) for 2 h to give a dark green solution. Concentration of the solution and workup as above gave the complex as a green microcrystalline solid. Yield: 0.111 g (90%). Anal. Calcd for $C_{42}H_{54}F_6N_2Ir_4PS_4Tl$: C, 27.51; H, 2.97; N, 1.53. Found: C, 27.32; H, 2.90; N, 1.52. MS (FAB+, $CH_2Cl_2$, *m*/*z*): 1689 ($TlIr_4(pyS_2)_2(cod)_4^+$, 100), 1485 ($Ir_4(pyS_2)_2(cod)_4^+$, 45). $\Lambda_M$ ($\Omega^{-1}$ cm$^2$ mol$^{-1}$): 126 (acetone, $4.98 \times 10^{-4}$ M). $^1$H NMR ($CD_2Cl_2$, 293 K) $\delta$: 7.15 (d, 2H, $J_{H-H}$ = 7.8 Hz), 6.76 (t, 4H, $J_{H-H}$ = 7.8 Hz) ($pyS_2$), 5.50 (m, 4H, =CH), 4.70 (m, 2H, =CH), 4.55 (m, 4H, =CH), 4.20 (m, 4H, =CH), 4.00 (m, 2H, =CH), 3.05 (m, 6H, >$CH_2$), 2.80−2.05 (m, 26H, >$CH_2$) (cod).

**Crystal Structure Determination of $[TlRh_4(\mu\text{-}pyS_2)_2(cod)_4][PF_6]\cdot CH_2Cl_2$ ($3\cdot CH_2Cl_2$).** A summary of crystal data and refinement parameters is given in Table 2. Suitable crystals for X-ray diffraction were obtained by diffusion of hexane into a dichloromethane−acetone solution of **3**. A brown irregular block of approximate dimensions 0.12 × 0.23 × 0.38 mm was mounted on the top of a glass fiber. Diffraction data were recorded on a Siemens-Stoe AED-2 diffractometer using graphite-monochromated Mo Kα radiation ($\lambda$ = 0.71073 Å). Cell constants were obtained from the least-squares fit on the setting angles of 58 reflections in the range $24° \le 2\theta \le 38°$. A total of 17 212 reflections with $2\theta$ in the range 3−50° ($\pm h, +k, \pm l$) were measured using the $\omega/2\theta$ scan technique and corrected for Lorentz and polarization effects. A semiempirical absorption correction, based on azimuthal $\psi$-scans from 12 reflections, was also applied (minimum and maximum transmission factors are 0.643 and 0.837).[40] A total of 9826 unique reflections were used in the refinement ($R_{int}$ = 0.0397). Three standard reflections were monitored every 55 min as a check of crystal and instrument stability; no important variation was observed.

**Table 2.** Crystallographic Data for $[TlRh_4(\mu\text{-}pyS_2)_2(cod)_4][PF_6]\cdot CH_2Cl_2$ ($3\cdot CH_2Cl_2$)

| | |
|---|---|
| empirical formula | $C_{42}H_{54}F_6N_2PRh_4S_4Tl\cdot CH_2Cl_2$ |
| fw | 1561.02 |
| temp, K | 173(2) |
| space group | $P2_1/c$ (No. 14) |
| *a*, Å | 12.650(2) |
| *b*, Å | 21.262(4) |
| *c*, Å | 21.090(4) |
| $\beta$, deg | 99.160(4) |
| *V*, Å$^3$ | 5600.1(17) |
| *Z* | 4 |
| $\rho$(calcd), g cm$^{-3}$ | 1.851 |
| $\mu$(Mo Kα), mm$^{-1}$ | 4.345 |
| data/restraints/parameters | 9826/13/588 |
| $R(F)$ [$F^2 > 2\sigma(F^2)$][a] | 0.0476 |
| $wR(F^2)$ [all data][b] | 0.1219 |

[a] $R(F) = \sum||F_o| - |F_c||/\sum|F_o|$, for 6751 observed reflections. [b] $wR(F^2) = (\sum[w(F_o^2 - F_c^2)^2]/\sum[w(F_o^2)^2])^{1/2}$.

The structure was solved by direct methods (SIR92)[41] and difference Fourier techniques and refined by full-matrix least-squares on $F^2$ (SHELXL97),[42] first with isotropic and then with anisotropic displacement parameters for all non-hydrogen atoms. Hydrogen atoms were introduced in calculated positions or located in a difference Fourier map (those bonded to olefinic carbons) and refined riding on the corresponding carbon atoms. At this stage, a difference Fourier map showed the presence of a heavily disordered solvent molecule with peaks up to 4.19 e Å$^{-3}$. This feature was modeled as one dichloromethane molecule disordered over four positions; each $CH_2Cl_2$ moiety was refined with restrained geometry and two common isotropic displacement factors for chlorine and carbon atoms. The following weighting scheme was used: $\omega = 1/[\sigma^2(F_o^2) + (xP)^2 + yP]$ ($P = (F_o^2 + 2F_c^2)/3$) with $x$ = 0.0461 and $y$ = 23.4586. The largest residual electron density was 1.31 e Å$^{-3}$, and was close to the disordered solvent. Atomic scattering factors, corrected for anomalous dispersion, were used as implemented in the refinement program.

**Acknowledgment.** Financial support from DGICYT (Projects PB95-221-C1 and PB94-1186) and a fellowship from Diputación General de Aragón (M. A. Casado) are gratefully acknowledged. We thank Dr. Agustín Sánchez (Inorganic Chemistry Department, University of Santiago de Compostela, Spain) for recording the $^{205}$Tl NMR spectra and Dra. Rosa I. Merino (Instituto de Ciencia de Materiales de Aragón) for recording the electronic absorption and emission spectra. We also thank Prof. P. Pyykkö for helpful discussions.

**Supporting Information Available:** An X-ray crystallographic file, in CIF format, for complex **3** is available. This material is available free of charge via the Internet at http://pubs.acs.org.

IC980988M

(40) North, A. C. T.; Phillips, D. C.; Mathews, F. S. *Acta Crystallogr.* **1968**, *A24*, 351.
(41) Altomare, A.; Cascarano, G.; Giacovazzo, C.; Guagliardi, A. *J. Appl. Crystallogr.* **1994**, *27*, 435.
(42) Sheldrick, G. M. *SHELXL-97*; University of Göttingen: Göttingen, Germany, 1997.